Biol. Cell (2014) **106,** 203–218 DOI: 10.1111/boc.201400014

Research article

Revelation of fibroblast protein commonalities and differences and their possible roles in wound healing and tumourigenesis using co-culture models of cells

Karla Jarkovska*[1], Barbora Dvorankova†[1], Petr Halada‡, Ondrej Kodet†, Pavol Szabo†, Suresh Jivan Gadher§, Jan Motlik*, Hana Kovarova*[2] and Karel Smetana Jr.†

*Institute of Animal Physiology and Genetics, Academy of Sciences of the Czech Republic., Libechov, Czech Republic, †Institute of Anatomy, First Faculty of Medicine, Charles University, Prague, Czech Republic, ‡Institute of Microbiology, Academy of Sciences of the Czech Republic, Prague, Czech Republic, and §Life Technologies, Frederick, MD, USA

Background information. The *in vitro* co-culture models of communication between normal fibroblasts and epithelial cells, such as keratinocytes or squamous cell carcinoma cells of FaDu line representing wound healing or cancer development, were established by non-direct contact between the cells and utilised in this study to examine epithelia-induced changes in overall fibroblast proteome patterns.

Results. We were able to select the proteins co-regulated in both models in order to evaluate possible molecular commonalities between wound healing and tumour development. Amongst the most pronounced were the proteins implemented in contractile activity and formation of actin cytoskeleton such as caldesmon, calponin-2, myosin regulatory light-chain 12A and cofilin-1, which were expressed independently of the presence of α-smooth muscle actin. Additionally, proteins altered differently highlighted functional and cellular phenotypes during transition of fibroblasts towards myofibroblasts or cancer-associated fibroblasts. Results showed coordinated regulation of cytoskeleton proteins selective for wound healing which were lost in tumourigenesis model. Vimentin bridged this group of proteins with other regulated proteins in human fibroblasts involved in protein or RNA processing and metabolic regulation.

Conclusions. The findings provide strong support for crucial role of stromal microenvironment in wound healing and tumourigenesis. In particular, epithelia-induced protein changes in fibroblasts offer new potential targets which may lead to novel tailored cancer therapeutic strategies.

Additional supporting information may be found in the online version of this article at the publisher's web-site

[1]These authors contributed equally to the study.
[2]To whom correspondence should be addressed (e-mail kovarova@iapg.cas.cz)

Key words: Cancer-associated fibroblasts, Contractile proteins, Myofibroblasts, Tissue injury, Tumourigenesis.

Abbreviations used: ANOVA, analysis of variance; 2D-E, two-dimensional electrophoresis; α-SMA, α-smooth muscle actin; CAFs, cancer-associated fibroblasts; CALD1, caldesmon; CAPG, macrophage-capping protein; CHAPS, 3–3(cholamidolpropyl)-dimethylammonio-1-propane sulphonate; CNN2, calponin-2; COF1, cofilin-1; COF2, cofilin-2; DTT, dithiothreitol; ECM, extracellular matrix; ENOA, α-enolase; ENPL, endoplasmin; G3P, glyceraldehyde-3-phosphate dehydrogenase; HFs, human fibroblasts; HKs, human keratinocytes; IEF, isoelectric focussing; LASP1, LIM and SH3 domain protein 1; ML12A, myosin regulatory light-chain 12A; MS, mass spectrometry; MFs, myofibroblasts; PDLI1, PDZ and LIM domain protein 1; PSA2, proteasome subunit alpha type-2; SCC, squamous cell carcinoma; SCCFs, squamous cell carcinoma fibroblasts; TCPB, T-complex protein 1 subunit beta; TPIS, triosephosphate isomerase; VIME, vimentin

Introduction

Organogenesis during embryonic development and tissue repair in adult mammals, like cancer development and progression, are both known to be regulated by interactions between epithelial cells, stromal cells, and components of the extracellular matrix (ECM). Similarly, we are becoming increasingly aware of the role of various molecular components in tissue repair and homeostasis.

The stromal cells such as fibroblasts secrete numerous ECM components including collagens, elastin, fibronectin, hyaluronic acid and various proteoglycans and glycoproteins, which make up the scaffold upon and in which cells reside, but also where ECM and ECM-related molecules together direct cell functions. In contrast to the physiological role of stroma in maintaining tissue homeostasis, stromal cells can also increase proliferation and production of ECM molecules under trauma such as tissue injury and resultant wound healing or during tumourigenesis (Smetana et al., 2013).

The stromal microenvironment plays a crucial role in tumour development and progression by inducing sustained epithelial hyperproliferation, metastasising of local tumour cells and enhancing angiogenesis (Polyak et al., 2009; Plzak et al., 2010; Valach et al., 2012). Tumour stroma contains cancer-associated fibroblasts (CAFs) with cancer supporting properties and frequently expressing α-smooth muscle actin (α-SMA) and/or vimentin (VME) bearing a resemblance to myofibroblasts (MFs) responsible for wound contraction (Gravina et al., 2013). Although the origin of CAFs is not fully clarified, they have a remarkable biological activity towards cancer epithelium, where they influence the expression of differentiation-dependent cell markers together with migration (De Wever et al., 2008; Haviv et al., 2009).

In our previous studies, we demonstrated that human fibroblasts (HFs) isolated from squamous cell carcinoma (SCC) of the head and neck can influence normal keratinocytes as judged by their differentiation pattern and epithelial–mesenchymal transition (Lacina et al., 2007; Strnad et al., 2010). In order to evaluate the possible paracrine effect of cancer cells on surrounding local HFs in acquiring the activity of CAFs, we co-cultured SCC cell line FaDu with normal fibroblasts, with resultant strong upregulation of IL-6, IL-8 and CXCL-1 transcripts in HFs and secretion of these cytokines in the co-culture media. Additionally, the same cytokines/chemokines were significantly upregulated in clinical SCC samples when compared with the paired normal mucosae. Interestingly, even normal human keratinocytes (HKs) were capable of influencing normal HFs as observed by upregulation of IL-6, IL-8 and CXCL-1 production (Kolar et al., 2012).

The well established *in vitro* co-culture models of (i) cross-talk between normal fibroblasts and keratinocytes (HF/HK) representing wound healing and (ii) cross-talk between normal fibroblasts and SCC cell line FaDu (HF/FaDu) representing cancer development were utilised in this study. The main aim was to compare the effects of normal or malignant epithelial cells on normal HFs at overall protein level, that is, proteomes (Figure 1). Using such an approach, we were able to select proteins that were co-regulated in both these study models in order to evaluate possible biological functionalities and similarities between wound healing and cancer development. In addition, our aim was to further study any protein alterations in individual models that may provide evidence of distinct functional and cellular phenotype involvement during transition of HFs towards MFs or CAFs.

Results

The protein fingerprints in HFs influenced by epithelial cells

The lysates of fibroblasts from 21-day cultures of HFs alone, HF/HK and HF/FaDu were subjected to two-dimensional electrophoresis (2D-E) and the protein maps for all 18 analysed samples (six biological replicates per sample group) were obtained. Redfin software was used for computer evaluation of protein maps to: (i) generate a composite image of all 2D maps, assign spot borders to each spot in gel images and quantify volumes of the detected spots; (ii) normalise spot quantitative data and apply statistical analysis using one-way analysis of variance (ANOVA) to select the protein spots significantly different between studied groups.

The evaluation of gel images provided in average 1027 and 463 protein spots for pH ranges 4–7 and 6–9, respectively. Representative images are shown in Figure 2, where in total 37 significantly

Figure 1 | Schematic representation of the study workflow
Human fibroblasts (HFs) were cultured alone or co-cultured in the presence of (i) human keratinocytes (HF/HK) and (ii) FaDu cell line (HF/FaDu). The lysates were subjected to 2D-E in two different pH ranges and the resulting protein maps were analysed using Redfin Solo software with a follow-up statistical analysis. The differentially expressed proteins were identified using MALDI-TOF/TOF MS and several of them were chosen for data verification and/or computer modelling of protein interactions for their enhanced functionality interpretation.

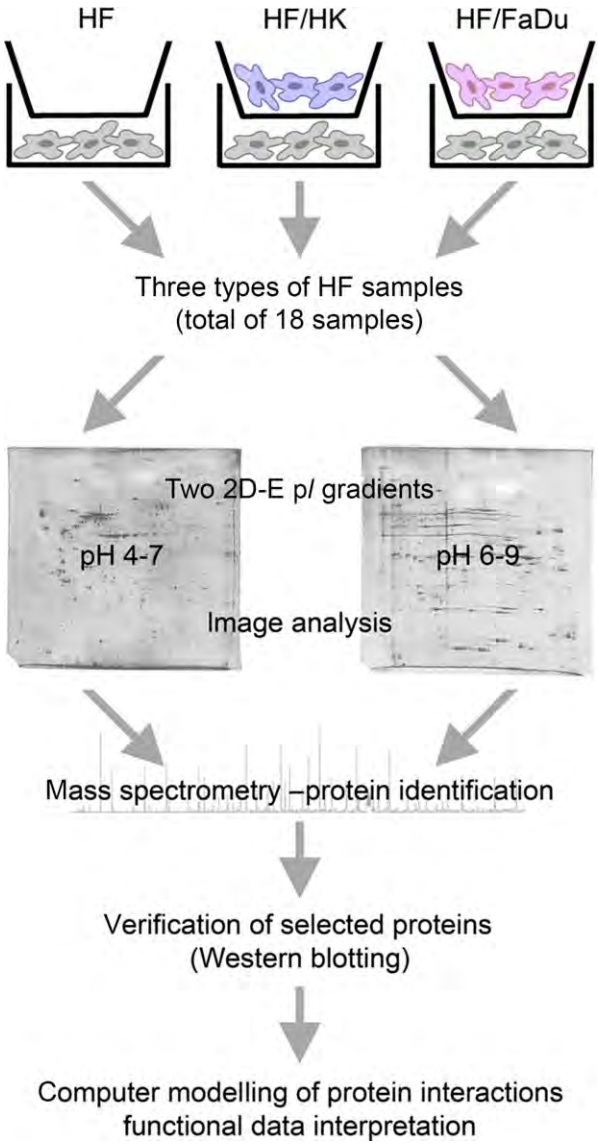

Figure 2 | Representative 2D-E gels of HF samples
Protein lysates of all three sample types were subjected to 2D-E, the resulting gels were stained using Sypro Ruby and analysed using Redfin solo software. Representative protein maps are shown for both 4–7 (**A**) and 6–9 (**B**) pH ranges. Differentially expressed spots were assigned by the data analysis software and are depicted in white with an arrow and with a "b" suffix for spots in pH range 6–9.

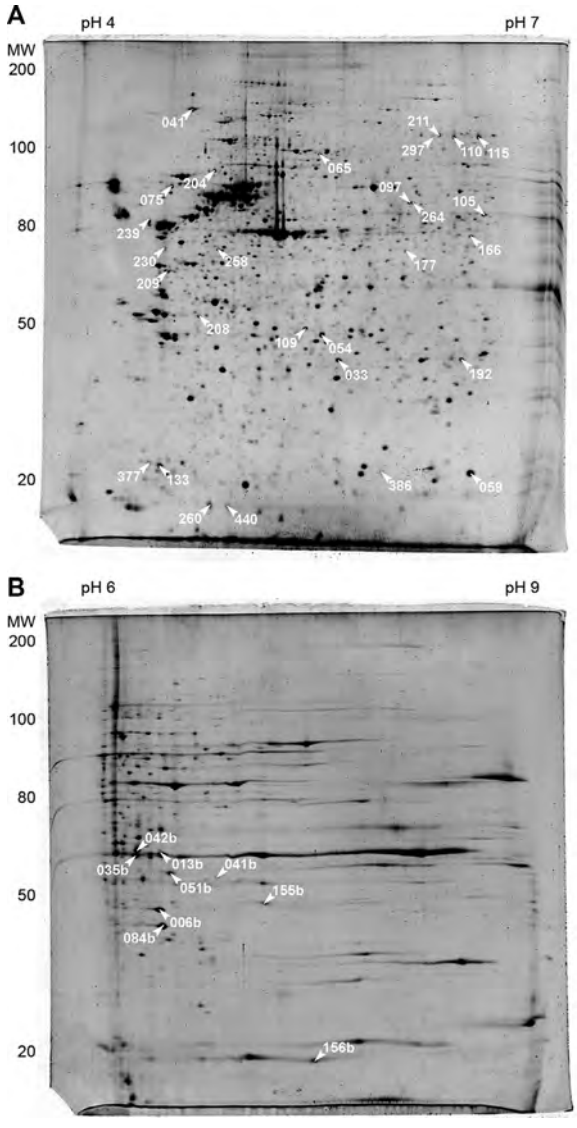

different protein spots ($P < 0.05$) in both pH ranges are indicated by a white arrow and a number assigned by the evaluation software. A detailed view of these spots including their positions on 2D gel, histograms showing normalised volumes of each spot in individual cell samples, and fold change calculated from the mean normalised volumes between compared groups as well as P values given for the changes among three studied sample groups is documented in

Supplementary Figures S1 and S2 for pH gradient 4–7 and 6–9, respectively. The proteins identified from spots using mass spectrometry (MS), represented in total 27 unique proteins (Table 1, details of the MS analysis data in Supplementary Tables S1 and S2). To note, there were several proteins present in more than one spot including: β-actin (ACTB; spot No. 054, 208, 260 and 440); caldesmon (CALD1; spot No. 110, 115, 211 and 297); endoplasmin (ENPL; spot No. 075, 204, 209 and 258); myosin regulatory light-chain 12A (ML12A; spot No. 133 and 377), glyceraldehyde-3-phosphate dehydrogenase (G3P; spot No. 041b, 155b) and triosephosphate isomerase (TPIS; No. 192, 006b). These observations highlight the capability of 2D-E to separate protein species of individual proteins which are very often present because of the post-translational modifications, alternative splicing or protein fragmentation. There were four spots (No. 035b, 042b, 054 and 258) containing two proteins in one spot, hence it was difficult to distinguish which of the proteins present contributed to the observed quantitative changes (Table 1).

In addition to ANOVA which is capable of comparing multiple groups and underlying the significance and fold change for the biggest difference, we extended data evaluation by applying *t*-test for comparison of two groups, for example, HF versus HF/HK or HF versus HF/FaDu, in order to accurately allow selection of proteins which were significantly influenced in the same direction of regulation and hence co-regulated in both co-culture models (Table 1A and B) or influenced differently with distinction of the two models (Table 1C and D).

Co-regulated protein changes in HFs co-cultured with either normal or cancer epithelial cells

Amongst the most pronounced changes in HFs as classified by significance and fold change were those proteins which were co-regulated in HFs co-cultured either with normal or cancer epithelial cells (Table 1A and B). They included increases in the levels of the proteins such as CALD1 (spot 115, the most basic spot – see Figure 4A), cofilin-1 (COF1), T-complex protein 1 subunit beta (TCPB) and ML12A (Table 1A). This also included proteins which were decreased very similarly in HFs co-cultured either with normal or cancer epithelial cells including CALD1 (297 and 110), ENPL (spot 041 corresponding to whole protein form), TPIS (006b), proteasome subunit alpha type-2 (PSA2; 084b), calponin-2 (CNN2; 013b) and heat shock protein beta-1 (HSPB1; 033) (Table 1B).

Different protein changes in HFs co-cultured with normal or cancer epithelial cells

Data identified a group of proteins which were significantly increased or decreased in HFs co-cultured with normal keratinocytes but not with cancer epithelial FaDu cells (Table 1C). Significantly higher levels of α-enolase (ENOA; 166) and reticulocalbin-3 (RCN3; 239) were observed followed by proteasome activator complex subunit 2 (PSME2; 109) and three ENPL spots (209, 075 and 204) present as fragments. Several increased ACTB fragments (260, 440 and 208) were also noticed. The levels of proteins including VIME (230), cofilin-2 (COF2; 386) and macrophage-capping protein (CAPG; 177) were significantly decreased in HF/HK only. Similarly, heterogeneous nuclear ribonucleoproteins H1 and H2 (HNRH1 and HNRH2, 097 and 264), ribose-phosphate pyrophosphokinase1 (PRPS1, 051b), heat shock 70 kD protein 1A/1B (HSP71, 065) and peptidyl-prolyl *cis–trans* isomerase A (PPIA, 156b) were observed to be significantly lower in HF/HK. Interestingly, not many protein changes in HFs co-cultured with cancer epithelial FaDu cells were observed (Table 1D).

Verification of selected protein changes using Western blot

Amongst alterations observed using 2-DE in HFs co-cultured with HKs or FaDu cells for 21 days, the most significant changes were reached by CALD1 including increase in basic spot 115, whilst decreases in two more acidic spots, namely 297 and 110, were observed (Table 1A and B and Figure 4A). Western blot of total CALD1 level on 21 day of co-culture showed a decrease, and similarly S789-phospho-CALD1 (S789-CALD1) form was lower in both HF/HK and HF/FaDu compared with HF alone (Figure 3A).

CNN2, showed a decrease on 2D-E in HFs co-cultured with HKs or FaDu on day 21 of co-culture (Table 1B). Western blot confirmed this downregulation only in HFs co-cultured with FaDu at the same time interval (Figure 3B), although the decrease

Table 1 | List of significant protein changes in HFs influenced by human keratinocytes (HF/HK) or cancer epithelial cells FaDu (HF/FaDu)

			ANOVA		*t*-Test HF/HK:HF		*t*-Test HF/FaDu:HF	
Spot	Protein name	DTB No.	*P* value	Fold change	*P* value	Fold change	*P* value	Fold change
(A) Proteins upregulated in both HF/HK and HF/FaDu models								
059	Cofilin-1	COF1_HUMAN	0.002	38.15	0.004	↑ 28.76	0.015	↑ 38.15
115	Caldesmon	CALD1_HUMAN	2.92E−05	16.47	2.22E−05	↑ 14.67	1.66E−04	↑ 16.47
105	T-complex protein 1 subunit beta	TCPB_HUMAN	0.003	15.82	2.81E−05	↑ 15.82	0.029	↑ 13.81
054	Prohibitin	PHB_HUMAN	0.004	1.81	0.017	↑ 1.81	0.003	↑ 1.40
	Actin, cytoplasmic 1[a)]	ACTB_HUMAN						
377	Myosin regulatory light-chain 12A	ML12A_HUMAN	0.011	1.60	0.009	↑ 1.60	0.039	↑ 1.28
133	Myosin regulatory light-chain 12A	ML12A_HUMAN	0.027	1.55	0.019	↑ 1.55	0.034	↑ 1.36
(B) Proteins downregulated in both HF/HK and HF/FaDu models								
297	Caldesmon	CALD1_HUMAN	0.001	2.13	0.002	↓ 0.47	0.005	↓ 0.59
042b	PDZ and LIM domain protein 1	PDLI1_HUMAN	0.006	1.93	0.008	↓ 0.52	0.008	↓ 0.54
	LIM and SH3 domain protein 1	LASP1_HUMAN						
110	Caldesmon	CALD1_HUMAN	0.034	1.74	0.032	↓ 0.59	0.030	↓ 0.57
035b	Annexin A2	ANXA2_HUMAN	0.023	1.69	0.009	↓ 0.59	0.022	↓ 0.60
	LIM and SH3 domain protein 1	LASP1_HUMAN						
006b	Triosephosphate isomerase	TPIS_HUMAN	0.013	1.66	0.024	↓ 0.74	0.003	↓ 0.60
033	Heat shock protein beta-1	HSPB1_HUMAN	0.016	1.62	0.014	↓ 0.62	0.026	↓ 0.70
041	Endoplasmin	ENPL_HUMAN	0.006	1.56	0.005	↓ 0.64	0.003	↓ 0.69
084b	Proteasome subunit alpha type-2	PSA2_HUMAN	0.015	1.56	0.038	↓ 0.76	0.010	↓ 0.64
013b	Calponin-2	CNN2_HUMAN	0.027	1.52	0.025	↓ 0.67	0.015	↓ 0.66
(C) Proteins with significantly different regulation in HF/HK model								
166	α-Enolase	ENOA_HUMAN	0.030	24.28	0.001	↑ 24.21	0.057	↑ 24.28
192	Triosephosphate isomerase	TPIS_HUMAN	0.003	3.60	0.004	↑ 3.60	0.095	↑ 1.73
260	Actin, cytoplasmic 1[b)]	ACTB_HUMAN	0.001	3.02	0.004	↑ 3.02	0.107	↑ 1.46
041b	Glyceraldehyde-3-phosphate dehydrogenase	G3P_HUMAN	0.046	2.66	0.027	↑ 2.66	0.227	↑ 1.25
440	Actin, cytoplasmic 1	ACTB_HUMAN	0.013	2.46	0.004	↑ 2.46	0.167	↑ 1.45
239	Reticulocalbin-3	RCN3_HUMAN	4.57E-04	2.20	4.24E-04	↑ 2.20	0.059	↑ 1.30
208	Actin, cytoplasmic 1	ACTB_HUMAN	0.024	2.01	0.019	↑ 2.01	0.233	↑ 1.21
109	Proteasome activator complex subunit 2	PSME2_HUMAN	0.005	1.81	0.004	↑ 1.81	0.051	↑ 1.28
209	Endoplasmin[a)]	ENPL_HUMAN	0.002	2.07	0.004	↑ 2.05	0.458	→ 0.99
075	Endoplasmin[b)]	ENPL_HUMAN	0.019	1.85	0.022	↑ 1.60	0.265	→ 0.87
204	Endoplasmin[b)]	ENPL_HUMAN	0.007	1.75	0.018	↑ 1.48	0.187	→ 0.85
258	Heterogeneous nuclear ribonucleoproteins C1/C2	HNRPC_HUMAN	0.002	1.64	0.003	↑ 1.64	0.301	→ 1.07
	Endoplasmin[2]	ENPL_HUMAN						
156b	Peptidyl-prolyl *cis–trans* isomerase A	PPIA_HUMAN	0.033	3.83	0.019	↓ 0.62	0.078	↑ 2.38
230	Vimentin	VIME_HUMAN	0.010	1.63	0.001	↓ 0.61	0.166	→ 0.89
177	Macrophage-capping protein	CAPG_HUMAN	0.028	1.68	0.018	↓ 0.60	0.126	→ 0.87
097	Heterogeneous nuclear ribonucleoprotein H	HNRH1_HUMAN	0.030	1.55	0.009	↓ 0.64	0.386	→ 0.96
051b	Ribose-phosphate pyrophosphokinase 1	PRPS1_HUMAN	0.006	2.48	0.006	↓ 0.40	0.148	→ 0.83
264	Heterogeneous nuclear ribonucleoprotein H2	HNRH2_HUMAN	0.012	1.90	0.002	↓ 0.53	0.193	→ 0.88
386	Cofilin-2	COF2_HUMAN	0.009	1.70	0.003	↓ 0.59	0.139	→ 0.90
065	Heat shock 70 kDa protein 1A/1B	HSP71_HUMAN	0.034	1.80	0.050	↓ 0.55	0.125	↓ 0.76
(D) Proteins with significantly different regulation in HF/FaDu model								
211	Caldesmon	CALD1_HUMAN	0.021	1.75	0.142	→ 0.85	0.016	↓ 0.57
155b	Glyceraldehyde-3-phosphate dehydrogenase	G3P_HUMAN	0.013	2.68	0.065	↓ 0.67	0.003	↓ 0.37

The table shows spot numbers generated by 2D-E data analysis software, protein name and its database accession in UniProtKB database. For all spots/proteins, the fold changes and p-values calculated by ANOVA analysis in Redfin software and followed-up by *t*-test are listed. The trend of change is depicted by direction of the arrow, where ↑ indicates increase higher than 1.2, ↓ means decrease below 0.8 and → shows no significant change with ratio between 0.8 and 1.2.

[a]C-terminal fragment.

[b]N-terminal fragment.

Figure 3 | Western blot analyses of selected proteins identified as differentially expressed in fibroblast samples
Protein lysates were subjected to 1D SDS-PAGE and transferred to a PVDF membrane, where protein-specific bands were detected using antibodies raised against caldesmon and S789-phospho-caldesmon (**A**), calponin-2 (**B**), α-enolase (**C**), LIM and SH3 domain protein 1 (LASP1; **D**) and PDZ and LIM domain protein 1 (PDLI1; **E**) proteins. For all proteins, a histogram of relevant spots from 2D-E is shown and is accompanied by a representative Western blot image of scanned CLXposure film and a dot-plot of the ratio of optical density for each protein normalised to a housekeeping protein β-tubulin intensity for monitoring of protein loading.

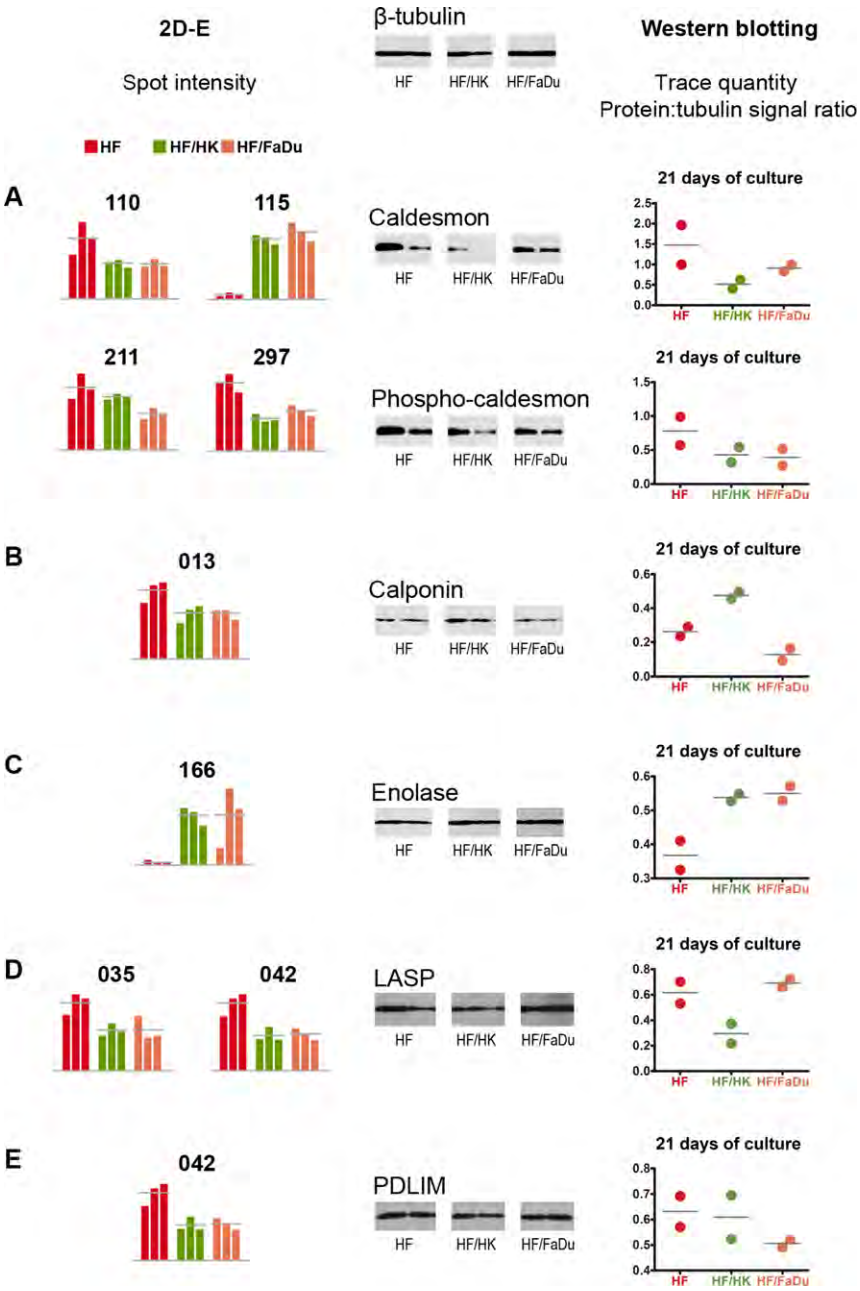

Figure 4 | Analysis of different protein species of caldesmon using 2D Western blot

(**A**) Caldesmon was identified in four different spots (115, 110, 211 and 297) using 2D-E suggesting the presence of post-translational modifications affecting p*I* of the species. Whilst the basic spot No. 115 was significantly increased, remaining three spots (110, 211 and 297) were decreased when HFs were co-cultured with HKs (HF/HK) or FaDu cells (HF/FaDu) compared with HFs alone. (**B**) Using specific antibodies to caldesmon and anti-S789-phospho-caldesmon in 2-D, Western blot analysis showed the most basic spot No. 115 being the least phosphorylated of all caldesmon spots in HFs. Reduced phosphorylation of caldesmon in HFs was also confirmed by immunofluorescence. (**C**) An increase of less phosphorylated caldesmon species was observed when SCCFs were co-cultured with FaDu (SCCF/FaDu) in comparison with SCCFs alone.

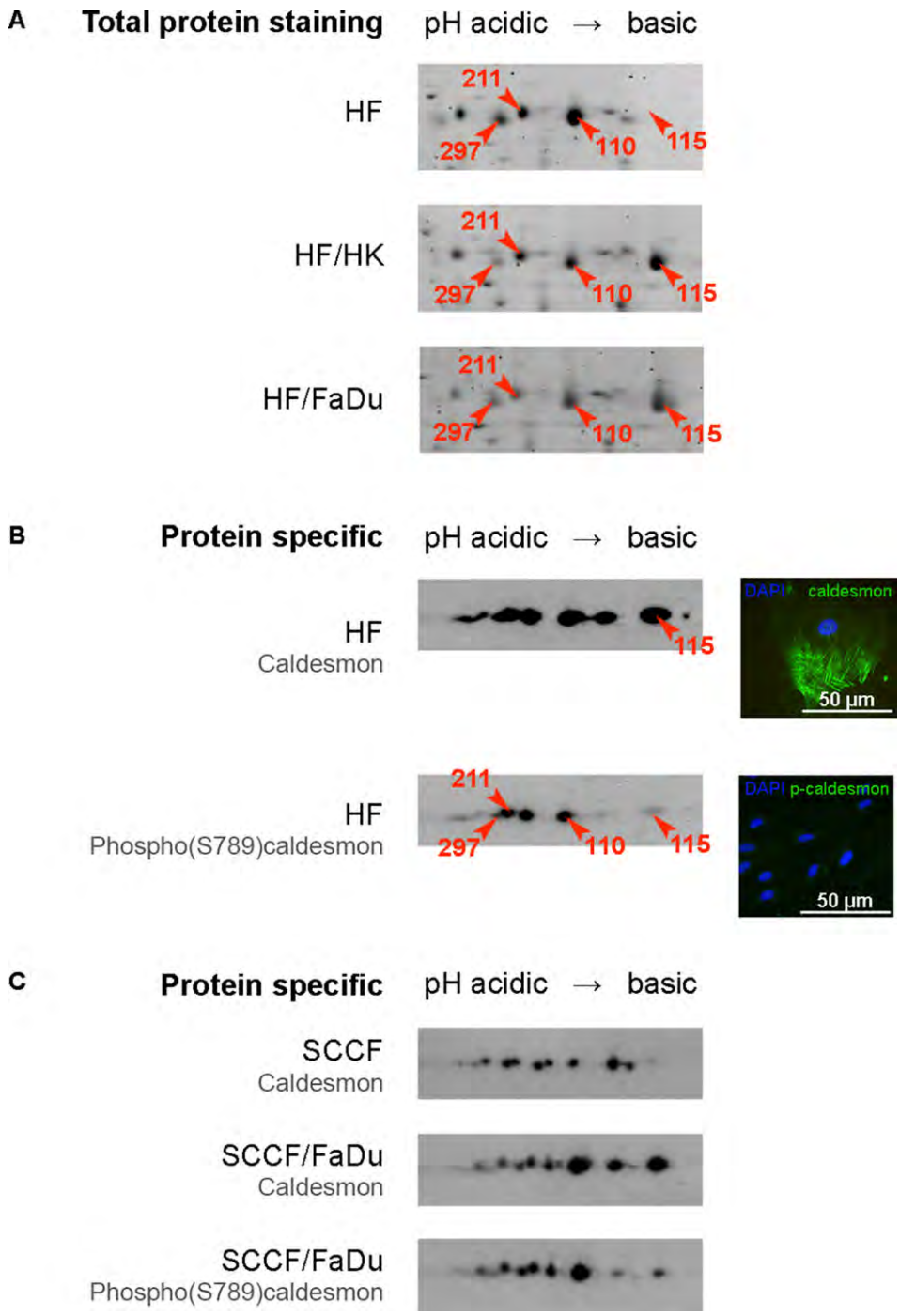

on day 7 of co-culture was more evident during co-culture of HFs with HKs as well as FaDu (not shown).

The considerable increase in ENOA in HF/HK on 21 day according to 2D-E (Table 1C) was proved by Western blot not only for HFs co-cultured with HKs but also in HFs under influence of FaDu cells (Figure 3C).

There were two protein spots (035 and 042), significantly different in HF/HK and HF/FaDu cultures according to 2D-E (Table 1B), each containing two proteins, hence careful elucidation of the protein contributing to the observed differences on 2D-E was necessary otherwise such spots/proteins could result in being excluded from data interpretation. Western blot indicated that in spot 035 containing annexin A2 and LIM and SH3 domain protein 1 (LASP1), it was LASP1 contributing to the observed decrease in HFs co-cultured with HKs (Figure 3D). As regards spot 042b, containing LASP1 and PDZ and LIM domain protein1 (PDLI1), Western blotting confirmed PDLI1 to be lower in HFs co-cultured with FaDu cells only compared with HFs alone (Figure 3E).

Although two biological replicates in each group of samples in Western blot analysis do not allow statistical evaluation, the trends of regulation evidently supported 2D-E findings.

Biological functions of proteins in HFs altered in the presence of epithelial cells

Based on the identity of the regulated proteins, it was possible using UniProtKB database to assign known biological functions to the proteins identified in HFs and influenced by epithelial cells. Exclusively in HFs co-cultured in conditions HF/HK as well as HF/FaDu was a group of proteins including CALD1, ML12A and CNN2 known to regulate contractile activity of the cells and also involved in cytoskeletal regulation like COF1 implemented in actin cytoskeleton dynamics. In addition, modulation of molecular chaperone proteins participating in cellular stress response (TCPB, HSPB1 and ENPL) highlighted another commonality to both studied models. Several proteins participating in glycolysis (TPIS) and proteasome regulation (PSA2) were also altered in HFs influenced by normal keratinocytes as well as cancer FaDu cells (Table 2A and B).

Among the proteins typically changed in HFs co-cultured with normal keratinocytes but not with cancer epithelial FaDu cells (Table 2B) was a group of proteins involved in actin cytoskeleton dynamics, namely COF2, LASP1 and CAPG, several actin fragments as well as known component of intermediate filaments, VIME. In addition, there were proteins implemented in protein processing (RCN3, HSP71 and PPIA) and RNA processing (HRNPH1/H2). Furthermore, we observed significant alterations in the levels of metabolic proteins TPIS involved in glycolysis and PRPS1 essential for nucleotide synthesis. Additionally, change in PSME2 implicated in immunoproteasome assembly and required for efficient antigen processing was also observed (Table 2C).

The normal as well as cancer epithelial cells mediate increase in low phosphorylated form of CALD1 in HFs

CALD1 was one of the most affected proteins in fibroblasts co-cultured with epithelial cells. On 2D-E, we identified four different protein spots belonging to this protein (Figure 4A). It was evident that the basic spot (No. 115) was increased in HF/HK and HF/FaDu conditions compared with HFs alone whilst three more acidic spots (Nos. 297, 110, 111) were decreased. Using immunospecific 2D Western blot with specific antibodies recognising either total CALD1 or S789-CALD1 phosphorylated form of this protein, we demonstrated that the increased basic form of CALD1 was the less phosphorylated form (Figure 4B). Reduced phosphorylation of CALD1 in HFs was also confirmed by immunofluorescence (Figure 4B). Importantly, similar regulation was also observed in squamous cell carcinoma fibroblasts (SCCFs) where increase in the basic but less phosphorylated CALD1 spot was evident in SCCF/FaDu co-culture (Figure 4C).

Interaction network connecting the proteins in HFs influenced by epithelial cells

In order to visualise possible interactions between proteins in HFs which were influenced in the presence of epithelial cells, computer modelling of interaction networks was utilised. UniProtKB accessions of the proteins from Table 1A and B were introduced into Interologous Interaction Database in order to evaluate direct or intermediate interactions of the co-regulated proteins in HFs co-cultured with either normal or cancer epithelial cells. Figure 5A depicts such interaction network generated by NAViGaTOR software. In total, 892

Table 2 | List of identified proteins and their biological functions

Protein name		DTB No.	Function
(A) Proteins upregulated in both HF/HK and HF/FaDu models			
Actin, cytoplasmic 1	(spot No. 054)	ACTB_HUMAN	Cytoskeleton
Caldesmon	(spot No. 115)	CALD1_HUMAN	Cytoskeleton – cellular component movement, muscle contraction
Cofilin-1		COF1_HUMAN	Cytoskeleton – actin cytoskeleton dynamics regulation
Myosin regulatory light-chain 12A		ML12A_HUMAN	Regulation of cell contractile activity
T-complex protein 1 subunit beta		TCPB_HUMAN	Molecular chaperon, *in vitro* plays a role in the folding of actin and tubulin
(B) Proteins downregulated in both HF/HK and HF/FaDu models			
Caldesmon	(spots No. 297, 110)	CALD1_HUMAN	Cytoskeleton – cellular component movement, muscle contraction
Calponin-2		CNN2_HUMAN	Cytoskeleton – smooth muscle contraction
Endoplasmin	(spot No. 041)	ENPL_HUMAN	Molecular chaperone involved in secretion
Heat shock protein beta-1		HSPB1_HUMAN	Molecular chaperone, stress response, actin organisation
Proteasome subunit alpha type-2		PSA2_HUMAN	Possibly regulator of proteasome
Triosephosphate isomerase	(spot No. 006b)	TPIS_HUMAN	Glycolysis, gluconeogenesis
(C) Proteins with significantly different regulation in HF/HK model			
Actin, cytoplasmic 1	(spots No. 260, 440, 208)	ACTB_HUMAN	Cytoskeleton
α-Enolase		ENOA_HUMAN	Glycolysis, plasminogen activation transcription regulation
Cofilin-2		COF2_HUMAN	Cytoskeleton – actin cytoskeleton dynamics regulation
Endoplasmin	(spots No. 209, 075, 204)	ENPL_HUMAN	Molecular chaperone involved in secretion
Glyceraldehyde-3-phosphate dehydrogenase	(spot No. 041b)	G3P_HUMAN	Glycolysis, regulation of translation, microtubule cytoskeleton organisation
Heat shock 70 kDa protein 1A/1B		HSP71_HUMAN	Molecular chaperone, stress response
Heterogeneous nuclear ribonucleoprotein H1		HNRH1_HUMAN	RNA processing
Heterogeneous nuclear ribonucleoprotein H2		HNRH2_HUMAN	RNA processing
LIM and SH3 domain protein 1		LASP1_HUMAN	Regulation of dynamic actin-based, cytoskeletal activities
Macrophage-capping protein		CAPG_HUMAN	Actin binding protein – reversibly blocks the barbed ends of actin filaments
Peptidyl-prolyl *cis–trans* isomerase A		PPIA_HUMAN	*cis–trans* isomerisation of proline imidic peptide bonds
Proteasome activator complex subunit 2		PSME2_HUMAN	Required for efficient antigen processing
Reticulocalbin-3		RCN3_HUMAN	*Endoplasmatic reticulum lumen*
Ribose-phosphate pyrophosphokinase 1		PRPS1_HUMAN	Catalyses the synthesis of phosphoribosylpyrophosphate
Triosephosphate isomerase	(spot No. 192)	TPIS_HUMAN	Glycolysis, gluconeogenesis
Vimentin		VIME_HUMAN	Cytoskeleton
(D) Proteins with significantly different regulation in HF/FaDu model			
Caldesmon	(spot No. 211)	CALD1_HUMAN	Cytoskeleton – cellular component movement, muscle contraction
Glyceraldehyde-3-phosphate dehydrogenase	(spot No. 155b)	G3P_HUMAN	Glycolysis, regulation of translation, microtubule cytoskeleton organisation
PDZ and LIM domain protein 1		PDLI1_HUMAN	Cytoskeletal adapter protein

The table shows spot numbers generated by 2D-E data analysis software, protein name and its database accession in UniProtKB database and the protein biological function(s) based on the information provided by UniProtKB database. For proteins identified in more than one spot, the numbers of individual spots corresponding to a species of a given protein are listed.

Figure 5 | Interaction networks generated by NAViGaTOR software

(**A**) UniProtKB accessions of the proteins from Table 1A and B were introduced into Interologous Interaction Database in order to evaluate direct or intermediate interactions of the co-regulated proteins in HFs co-cultured with either normal or cancer epithelial cells. Such modelling not only separated contractile proteins (CALD1, CNN2 and ML12A) from major part of interaction network but also exhibited their hierarchical importance in fibroblast transition to MFs as well as CAFs. (**B**) UniProtKB accessions of the proteins from Table 1C were introduced into Interologous Interaction Database in order to evaluate direct or intermediate interactions of the proteins typical for HFs influenced by normal HKs. The intermediate filament protein VIME was mainly responsible for interconnectivity via indirect interaction with proteins implemented in protein processing/stress response, RNA processing and metabolic pathways. Another proteins (COF-2, LASP1 and CAPG) involved mainly in actin cytoskeleton organisation appeared to be typical for HF/HK model of wound healing.

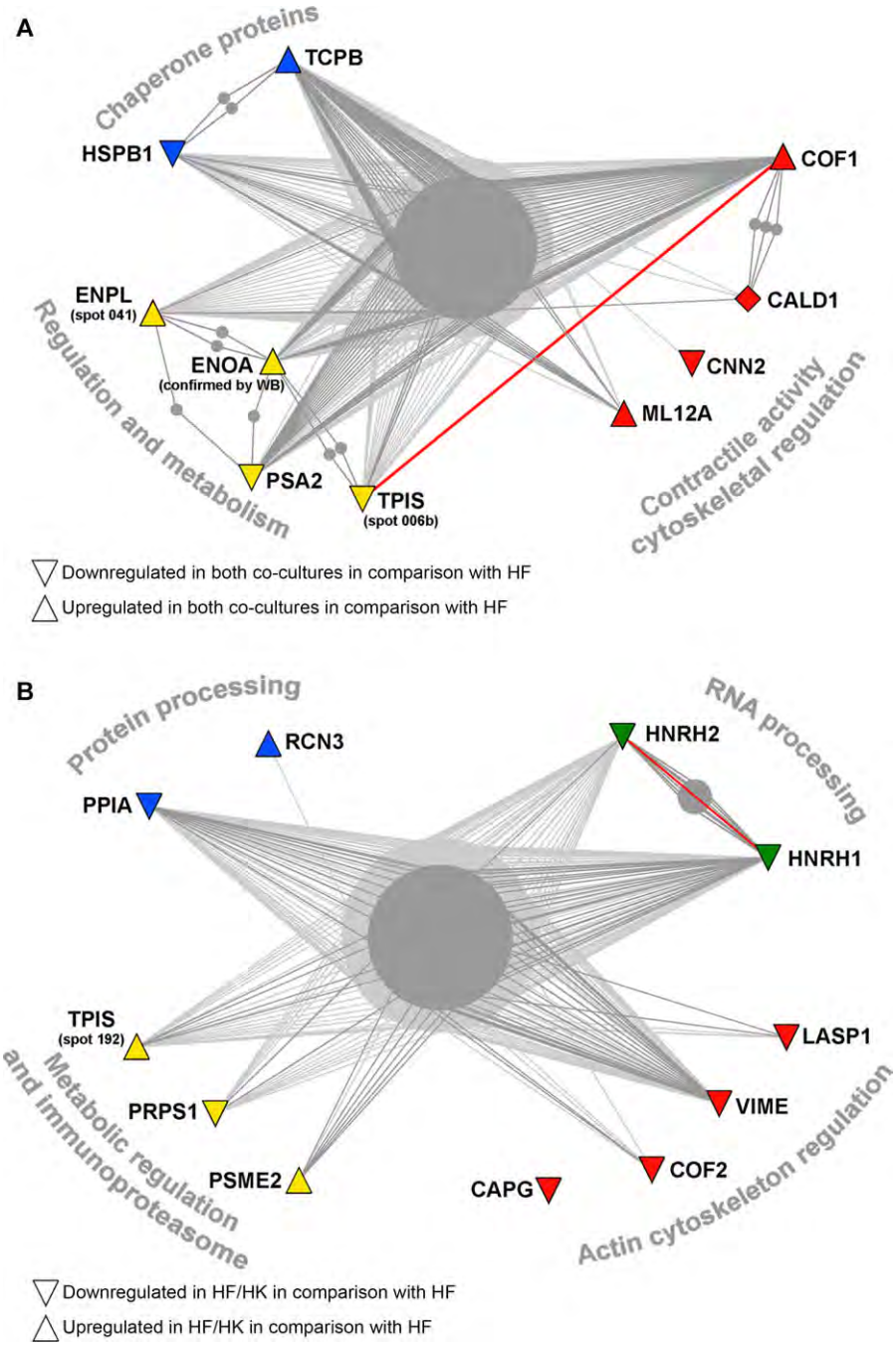

interactions were recognised for this group of proteins. Computer modelling highlighted a high number of mediated interactions mainly among COF1, TCPB and PSA2 proteins thus connecting biological processes of cytoskeletal organisation, stress response and metabolism/proteasome activity. Importantly, such modelling not only separated contractile proteins (CALD1, CNN2 and ML12A) from the interaction network but also exhibited their hierarchical importance in fibroblast transition to MFs as well as CAFs (Figure 5A).

Applying the same approach to evaluation of the proteins typical for HFs influenced by normal HKs (Table 1C), it was evident that intermediate filament protein VIME was mainly responsible for interconnectivity via indirect interaction with proteins implemented in protein processing/stress response, RNA processing and metabolic (glycolysis and nucleotide synthesis) pathways. In addition to VIME, another proteins (COF-2, LASP1 and CAPG) involved mainly in actin cytoskeleton organisation appeared to be typical for HF/HK model of wound healing (Figure 5B).

Discussion

Disruption of epithelial homeostasis is a common feature of tumourigenesis as well as of a wound which triggers response of surrounding stroma. In tumourigenesis, changes in the stroma are part of a whole process that drive invasion and metastasis, the hallmarks of malignancy. Stromal changes at the invasion front include the appearance of MFs and/or CAFs, the main precursors of which are fibroblasts (Otranto et al., 2012). The MFs play crucial role during wound healing too and transition of fibroblasts into MFs which assure ECM secretion and contractile activity is typical for proliferating and remodelling phases (Gabbiani et al., 1972). When a wound heals, MFs disappear via apoptosis, on the contrary if MFs persist, their activities change the wound into chronic site including developing fibrosis. Recently, it was suggested that tumour stroma environment is very similar to fibrotic tissue and CAFs adopt the ability to induce proliferation of epithelial cells and malignant transformation (Radisky et al., 2007). Our previous phenotype characterisation of HFs cultured in the presence of epithelial cells using immunocytochemistry showed no signal for contractile protein α-SMA in HFs alone or HF/HK co-culture, whilst FaDu cells triggered α-SMA expression in HFs and production of ECM. Despite such observed phenotypic difference between *in vitro* models of wound healing and tumour development in our models, upregulation of IL-6, IL-8 and CXCL-1 in dermal fibroblasts by HKs as well as FaDu cells, indicated certain degree of commonality of these two biologically relevant models of transition of HFs into MFs and CAFs. Simultaneous functional assays confirmed the importance of these factors in epithelial–mesenchymal communication (Kolar et al., 2012).

In this study, we accessed the proteins in HFs which may be responsible for the observed changes of fibroblasts, and verification of selected protein changes associated with studied phenotype models was performed using immune specific Western blot. The presented results point to the proteins which were co-regulated in HFs co-cultured with either normal or cancer epithelial cells. Among the most pronounced changes were the proteins implemented in contractile activity and formation of actin cytoskeleton such as CALD1, CNN-2, ML12A and COF1. CALD1 participates in the interaction of actin and myosin and its expression and function in MFs has been studied (Lazard et al., 1993; Kalekou et al., 2005; Hai and Gu, 2006; Council and Hameed, 2009; Huang et al., 2010; Leung et al., 2011; Salgueiredo-Giudice et al., 2011). Elevated expression of this protein was also observed in oral SCCs (Méndez et al., 2002) and its overexpression was associated with lymph node metastasis and poor prognosis in patients with oral cavity SCC (Chang et al., 2013). Additionally, it was shown that CALD1 phosphorylation reduced its binding to actin and myosin thus promoting pro-migratory and pro-invasive activities in breast cancer cells (Schwappacher et al., 2013). Hence, we hypothesised that de-phosphorylation of CALD1 in HFs co-cultured with HKs and FaDu cells or in SCCFs co-cultured with FaDu cells shown in this study may significantly contribute to contractile activity, promote formation of actin stress fibres and reduce cell motility during transition of fibroblast to MFs or CAFs.

We identified another protein, CNN2, known to bind to actin, troponin C, and tropomyosin which lead to the inhibition of actomyosin ATPase activity. Recently, it was shown that calponin-3, belonging to the same protein family, regulated stress fibre formation in dermal fibroblasts during wound

healing. Calponin-3 was associated with α-SMA in stress fibres formed by cultured dermal fibroblasts and its knockdown in primary fibroblasts resulted in a phenotype of decreased cellular dynamics such as cell motility and contractile ability (Daimon et al., 2013). Hence, the role of CNN2 may be analogous and it may extend the role of CALD1 discussed in previous paragraph.

COF1 is known to participate in actin polymerisation/depolymerisation and its expression and activation is tightly connected with myofibroblastic differentiation (Malmström et al., 2004; Zhao et al., 2007; Pho et al., 2008; Bosselut et al., 2010). Our study showed its additional role, demonstrating that COF1 was the major protein connecting via intermediated protein interactions actin fibre remodelling with other cellular processes such as stress response, energy metabolism and proteasome activity, which in turn are also modulated during MFs and CAFs differentiation. For example, folding of actin was related to activity of chaperone protein T-complex protein 1 (McCormack et al., 2009) and its activity during wound healing (Satish et al., 2010).

Besides common protein changes, this study also revealed the alterations which were selective for wound healing model and observed in HFs co-cultured with normal HKs but not tumour epithelial FaDu cells. Interestingly, the group of proteins involved in intermediate and actin filaments cytoskeletal functions (COF2, CAPG, LASP1 and VIME) showed downregulation in HFs in the presence of normal epithelial cells. Hence, wound healing model involves a very coordinated regulation of cytoskeleton proteins in HFs and it appears that this regulation is lost under influence of tumour epithelial cells. More importantly, VIME was seen to facilitate the connection of this group of proteins with other regulated proteins in HFs involved in protein or RNA processing, metabolic regulation and a immunoproteasome component.

ENOA was another protein that showed considerable increase in HFs under the influence of the normal HKs only. It is a multifunctional protein facilitating plasminogen activation to plasmin. This enzyme has the ability to degrade several components of ECM (Capello et al., 2011; Díaz-Ramos et al., 2012), suggesting that fibroblasts stimulated by epithelial cells may help remodel the ECM during wound healing. This modulation is lost in tumourigenesis model of HF/FaDu cells, leading to the unanswered question of its impact on early stages of tumour cell invasion and subsequent metastasis.

Our data showed that both types of epithelia-induced protein changes in normal HFs that may contribute to phenotypic conversion of HFs to MFs. Such events, even in the absence of α-SMA, may be responsible for wound contraction in healing. CAFs including MFs, frequently occurring in many types of malignancies, share part of the protein changes with wound healing MFs. These findings strongly support a hypothesis of commonality between the processes involved in wound healing and tumourigenesis based on the epithelial–mesenchymal communication. We conclude that normal and malignant keratinocytes commence the process of MF and/or CAFs formation in both wound healing and tumour growth with many similarities at protein level. This observation corroborates the hypothesis of Dvorak (1986) about similarities between tumour stroma generation and wound healing. It is also possible that wound and its chronic healing may play a role in cancer formation (Kowal-Vern and Criswell, 2005). Overall, epithelia-induced protein changes in fibroblasts offer new potential targets which may lead to novel anti-cancer therapeutic strategies.

Materials and methods

Chemicals

Acrylamide, bis-acrylamide, urea, Tris-base, thiourea, SDS, bromophenol blue, ammonium persulphate, tetramethylethylenediamine, n-octyl glucoside, Tris, (2-carboxyethyl) phosphine hydrochloride, iminodiacetic acid and iodoacetamide were obtained from Sigma. Nonidet-40, 3–3(cholamidolpropyl)-dimethylammonio-1-propane sulphonate (CHAPS) and dithiothreitol (DTT) were from USB Corporation. Instead of DeStreak reagent, bis(2-hydroxyethyl) disulphide (Alfa Aesar) was used. Tributyl-phosphine, and protein (Mini-Complete) and phosphatase (PhoStop) inhibitors cocktails were obtained from Roche. Immobiline DryStrip (18 cm, 4–7 and 6–9) and amholines pH 4–7 and pH 6–9 were purchased from GE Healthcare. Sypro Ruby Protein Gel was from Bio-Rad Laboratories. All other chemicals were of HPLC or analytical grade and buffers were prepared using Milli-Q water system (Millipore). Unless otherwise specified, all chemicals used for MS were from Sigma. Anti-CALD1, anti-S789-CALD1 anti-CNN2 antibodies were obtained from Abcam. Anti-β-tubulin, anti-ENOA, anti-LASP1 and anti-PDLI1 antibodies were purchased from Sigma–Aldrich. Peroxidase-conjugated secondary anti-rabbit or anti-mouse IgG antibodies were from Jackson Immunoresearch.

The Immobilon P membranes were purchased from Millipore and the ECL+ chemiluminiscence system from GE Healthcare.

Cell culture

Normal dermal HFs and normal interfollicular HKs were isolated from residual skin samples from plastic surgery, SCCFs were separated from the sample of SCC. All tissue samples and cells were collected after informed consent of donors according to the Helsinki Declaration. The process of isolation of single cell types was described in our previous studies (Strnad et al., 2010; Kolar et al., 2012). The commercially available FaDu cell line of a hypopharyngeal carcinoma was obtained from ATCC (No. HTB-43). *In vitro* model of the study was established by non-direct contact between epithelial cells (HK or FaDu) and normal dermal HFs using transwell system with 21 days of culturing. HFs were inoculated into three wells of six-well dish (Corning) at a density of 1000 cells/cm^2. They were cultured alone or co-cultured with epithelial cells, which were seeded into transwell insert system, with HK on collagen membrane (40,000 cells/cm^2) and FaDu on polyethylene terephthalate membrane (2000 cells/cm^2) (both Corning) (Figure 1). The density of epithelial cells was determined on the basis of growth kinetics for the distinct epithelial cell types. The cells were cultured in Dulbecco's modified Eagle's medium (Biochrom) with 10% fetal bovine serum (Biochrom) at 37°C and 5% CO_2 for 21 days. During this period, HFs were sub-cultured three times and the number of the wells was gradually increased to final number of 36 wells for each type of cell culture conditions (HF, HF/HK and HF/FaDu). During each sub-culture, new inserts with fresh epithelial cells were used. At the end of cultivation, culture medium was aspirated, HFs were washed four times with cold Dulbecco's PBS and 50 µl of lysis buffer [7 M urea, 2 M thiourea, 3% w/v CHAPS, 2% v/v Nonidet P-40 and 5 mM (2-carboxyethyl) phosphine hydrochloride] containing protease and phosphatase inhibitors was added to each well. The harvested cells were lysed at room temperature for 30 min and the lysates transferred to a tube (cells from 12 wells made one biological replicate), rapidly frozen in liquid nitrogen and stored at −80°C. The protein concentration of cell lysates was measured using Pierce 660 nm Protein Assay (Thermo Scientific) and the lysates were used for 2D-E studies. For Western blot verification of specific proteins, the cells were independently cultured under the same conditions for 21 days. The cells covering 30 cm^2 of the confluent cell growth were lysed using lysis buffer (7 M urea, 2 M thiourea, 3% w/v CHAPS, 2% v/v Nonidet P-40, 5 mM (2-carboxyethyl) phosphine hydrochloride) containing protease and phosphatase inhibitors and collected as one biological replicate.

With reference to our previous findings (Kodet et al., 2013; Szabo et al., 2013), cultures of SCCFs were set up and SCCFs were co-cultured with FaDu (SCCF/FaDu) for direct comparison with the fibroblast-epithelial co-cultivation model. HF, HF/HK, SCCF and SCCF/FaDU were cultured for 7 days and three biological replicates were prepared, each from 120 cm^2 of the confluent cell growth, for 2D Western blot analysis.

2D-E and image analysis

For 2D-E in pH 4–7 range, sample aliquots corresponding to 100 µg protein were processed as described previously by Hrabakova et al. (2013). Briefly, samples were loaded on the first dimension isoelectric focussing (IEF) for separation using active in gel rehydration of Immobiline DryStrips (18 cm pH 4–7), performed on IEF cell (Bio-Rad) system. After IEF separation, the gel strips were equilibrated in 6 M urea, 4% SDS, 30% glycerol, 50 mM Tris–HCl pH 8.8, 100 mM DeStreak reagent and bromophenol blue for 25 min, rinsed and transferred on vertical 12% SDS-PAGE (18 × 18 × 1 mm^3) gel. For 2D-E in pH 6–9 range, sample aliquots corresponding to 100 µg protein in lysis buffer with an addition of pH 6–9 ampholytes (0.5%, w/v), protease and phosphatase inhibitors (Roche), DTT, iodoacetamide and tributyl-phosphine were loaded on the first dimension IEF separation using cup-loading on Immobiline DryStrips (IPG strip, 18 cm pH 6–9) previously rehydrated using buffer containing 7 M urea, 2 M thiourea, 4% CHAPS, pH 6–9 ampholytes (0.5%, w/v), phosphatase and protease inhibitors, 30 mM DTT and 0.003% bromophenol blue (Hrabakova et al., 2013). After IEF separation, the gel strips were equilibrated in 6 M urea, 8% SDS, 30% glycerol, 50 mM Tris–HCl pH 8.8 and bromophenol blue for 20 min, rinsed and applied to vertical 12% SDS-PAGE (18 × 18 × 1 mm^3 gel) for the second dimension of 2D-E. SDS-PAGE was carried out at a constant current of 40 mA per gel using three in series connected Protean II xi Cells (Bio-Rad) allowing simultaneous run of six gels. Gels were then stained with fluorescent stain Sypro Ruby Protein Stain, scanned and digitised at 254 dpi resolution using a Pharos FX scanner (Bio-Rad).

The images were evaluated using Redfin Solo software (Ludesi; http://www.ludesi.com/redfin/). Gels were sorted into groups according to sample type (three groups – HF, HF/HK and HF/FaDu – each in pH ranges 4–7 and 6–9). Each sample group had six gels representing six biological replicates of a given sample. Following automatic spot detection and matching, data were normalised, that is, each protein spot was expressed as relative intensity of all valid spots, and normalised data were analysed using ANOVA available within the Redfin Solo. The protein spots with statistically different expression among three types of samples ($P < 0.05$) were selected for identification by MS.

For MS identification, preparative pH 4–7 gels were prepared with 500 µg protein load and stained using MS compatible zinc staining as previously described (Hardy and Castellanos-Serra, 2004; Hrabakova et al., 2013). The analytical gels pH 6–9 were directly stained with zinc staining and selected spots were excised.

Enzymatic digestion, MS and protein identification

Zinc-stained protein spots were excised from the gel, washed and digested with trypsin as described previously (Hrabakova et al., 2013). Mass spectra were acquired on Ultraflex III MALDI-TOF/TOF instrument (Bruker Daltonics) equipped with a LIFT^{TM} technology for MS/MS analysis. The mass spectra were searched against SwissProt 2013_08 database subset of human proteins using in-house MASCOT search engine with the following search settings: peptide tolerance of 30 ppm, missed cleavage site value set to one, variable carbamidomethylation of cysteine, oxidation of methionine and protein N-terminal acetylation. Proteins with MOWSE score over the threshold 56 calculated for the used settings were considered as identified. If the score was only slightly higher than the threshold value or the sequence coverage too low, the identity of the protein candidate was confirmed by MS/MS analysis.

Immunoblot and quantitative analysis

For 1D Western blot, independent samples of HFs from 21 day cultures of HF, HF/HK and HF/FaDu were used. Aliquots of the total protein extracts corresponding to 8 μg were separated in 12% SDS-PAGE gels (except for CALD1 and S789-CALD1 where 10% gels were used) on Mini PROTEAN® 3 system (Bio-Rad). Proteins were then transferred to Immobilon P (Millipore) membranes using a semi-dry blotting system (Biometra) and transfer buffer containing 48 mM Tris, 39 mM glycine and 20% methanol (except for CALD1 and phospho-CALD1, where 10% MeOH was used). The membranes were blocked for 1 h with 5% skimmed milk in Tris-buffered saline with 0.05% Tween 20 (pH 7.4) and incubated overnight with primary antibodies specific CALD1 (1:5000) and S789-CALD1 (1:1000), ENOA (1:60,000), CNN2 (1:2000), PDZ and LIM domain protein 1 (PDLI1; 1:2000) and LIM and SH3 domain protein 1 (LASP1; 1:15,000). The total protein load was monitored using anti-β-tubulin antibody (1:20,000). Peroxidase-conjugated secondary anti-rabbit or anti-mouse IgG antibodies were diluted 1:10,000 (except for enolase, where 1:20,000 dilution was used) in 5% skimmed milk in Tris-buffered saline with 0.05% Tween 20, and the ECL+ chemiluminiscence (GE Healthcare) detection system was used to detect specific proteins. The exposed CL-XPosure films (Thermo Scientific) were scanned using a calibrated densitometer GS-800 (Bio-Rad). The proteins bands of each sample were quantified as Trace Quantity (the quantity of a band as measured by the area under its intensity profile curve, units = intensity × mm) using Quantity One software (Bio-Rad). The phosphorylation pattern of CALD1 was studied using 2D Western blotting where both parts of the combination, 2D-E and the Western blotting shown in Figure 4, were performed.

Statistical analysis

Spot intensities of all differentially expressed spots were exported from Redfin Solo software into a csv file for further statistical analysis using Microsoft Excel 2007 (F-test; t-test). Normalised spot values for all three biological replicates were compared for HF versus HF/HK, and HF versus HF/FaDu. The data were tested for normality using F-test, followed by one-tailed t-test. Based on the F-test results, the settings were set as two-samples equal and unequal variance for F-test P values higher and lower than 0.05, respectively.

Computer modelling of protein interaction network

To analyse functional aspects including possible protein interactions among identified proteins and to reveal further as yet unspecified interacting partners, we used an Interologous Interaction Database (Brown and Jurisica, 2005) (I2D; version 1.95). This database version of both known and predicted protein–protein interactions contained 120,030 source interactions, 59,741 predicted interactions for human and is available online at http://ophid.utoronto.ca/ophidv2.201/. We entered a separately list of identified proteins from two models: (i) proteins differentially expressed in HF/HK only, (ii) proteins common for both HF/HK and HF/FaDu co-cultures. Search criteria for observing interactions were set to select human as target organism and graph viewer was set to output format. The final illustrations were exported and visualised using NAViGaTOR (Network Analysis, Visualisation & Graphing TORonto) software (http://ophid.utoronto.ca/navigator) version 2.1.13.

Immunocytochemistry

CALD1 as well as phospho-CALD1 in HFs were also visualised by immunofluorescence using antibodies described in Chemicals. The FITC-labelled swine anti-rabbit serum (DAKO) was used as a second step antibody. The antibodies were diluted as recommended by supplier. The nuclei were counterstained by 4′,6-diamidino-2-phenylindole (DAPI) (Sigma–Aldrich). The control of the specificity of reaction was performed by irrelevant antibody. The ECLIPSE, Nikon fluorescence microscope equipped with filter-blocks specific for FITC and DAPI and a Cool-1300Q CCD camera (Vosskühler) were used. Data were analysed by LUCIA 5.1 computer-assisted image analysis system (Laboratory Imaging).

Author contribution

K.J. and B.D. carried out the experimental work and data analysis and interpretation; P.H. carried out experimental work; O.K. and P.S. carried out experimental work; S.J.G. contributed to manuscript writing; J.M. contributed to concept and design of the research; H.K. carried out data interpretation and wrote the article; K.S. Jr. contributed to concept and design of the research, carried out experimental work and wrote the article.

Funding

This study was supported by the Charles University projects for support of Specific University Research, UNCE [No. 203401], PRVOUK-27, Grant Agency of Ministry of Health [project No. 13344]; projects from the European Regional Development Fund ExAM [No. CZ.1.05/2.1.00/03.0124] and BIOCEV [No. CZ.1.05/1.1.00/02.0109]; Institutional Research Projects RVO67985904 (IAPG AS CR,v.v.i.) and RVO61388971 (IMIC, AS CR,v.v.i.).

Conflict of interest statement

The authors have declared no conflict of interest.

References

Bosselut, N., Housset, C., Marcelo, P., Rey, C., Burmester, T., Vinh, J., Vaubourdolle, M., Cadoret, A. and Baudin, B. (2010) Distinct proteomic features of two fibrogenic liver cell populations: hepatic stellate cells and portal myofibroblasts. Proteomics **10**, 1017–1028

Brown, K.R. and Jurisica, I. (2005) Online predicted human interaction database. Bioinformatics **21**, 2076–2082

Capello, M., Ferri-Borgogno, S., Cappello, P. and Novelli, F. (2011) α-Enolase: a promising therapeutic and diagnostic tumor target. FEBS J. **278**, 1064–1074

Council, L. and Hameed, O. (2009) Differential expression of immunohistochemical markers in bladder smooth muscle and myofibroblasts, and the potential utility of desmin, smoothelin, and vimentin in staging of bladder carcinoma. Mod. Pathol. **22**, 639–650

Daimon, E., Shibukawa, Y. and Wada, Y. (2013) Calponin 3 regulates stress fiber formation in dermal fibroblasts during wound healing. Arch. Dermatol. Res. **305**, 571–584

Díaz-Ramos, A., Roig-Borrellas, A., García-Melero, A. and López-Alemany, R. (2012) α-Enolase, a multifunctional protein: its role on pathophysiological situations. J. Biomed. Biotechnol. **2012**, 156795

Dvorak, H.F. (1986) Tumors: wounds that do not heal. Similarities between tumor stroma generation and wound healing. N. Engl. J. Med. **315**, 1650–1659

Gabbiani, G., Hirschel, B.J., Ryan, G.B., Statkov, P.R. and Majno, G. (1972) Granulation tissue as a contractile organ. A study of structure and function. J. Exp. Med. **135**, 719–734

Gravina, G.L., Mancini, A., Ranieri, G., Di Pasquale, B., Marampon, F., Di Clemente, L., Ricevuto, E. and Festuccia, C. (2013) Phenotypic characterization of human prostatic stromal cells in primary cultures derived from human tissue samples. Int. J. Oncol. **42**, 2116–2122

Hai, C.-M. and Gu, Z. (2006) Caldesmon phosphorylation in actin cytoskeletal remodeling. Eur. J. Cell Biol. **85**, 305–309

Hardy, E. and Castellanos-Serra, L.R. (2004) "Reverse-staining" of biomolecules in electrophoresis gels: analytical and micropreparative applications. Anal. Biochem. **328**, 1–13

Haviv, I., Polyak, K., Qiu, W., Hu, M. and Campbell, I. (2009) Origin of carcinoma associated fibroblasts. Cell Cycle **8**, 589–595

Hrabakova, R., Kollareddy, M., Tyleckova, J., Halada, P., Hajduch, M., Gadher, S.J. and Kovarova, H. (2013) Cancer cell resistance to aurora kinase inhibitors: identification of novel targets for cancer therapy. J. Proteome Res. **12**, 455–469

Huang, R., Grabarek, Z. and Wang, C.-L.A. (2010) Differential effects of caldesmon on the intermediate conformational states of polymerizing actin. J. Biol. Chem. **285**, 71–79

Chang, K.-P., Wang, C.-L.A., Kao, H.-K., Liang, Y., Liu, S.-C., Huang, L.-L., Hseuh, C., Hsieh, Y.-J., Chien, K.-Y., Chang, Y.-S., Yu, J.-S. and Chi, L.-M. (2013) Overexpression of caldesmon is associated with lymph node metastasis and poorer prognosis in patients with oral cavity squamous cell carcinoma: Caldesmon overexpression in OSCC. Cancer **119**, 4003–4011

Kalekou, H., Kostopoulos, I., Milias, S. and Papadimitriou, C.S. (2005) Comparative study of CD34, alpha-SMA and h-caldesmon expression in the stroma of gynaecomastia and male breast carcinoma. Histopathology **47**, 74–81

Kodet, O., Dvořánková, B., Krejčí, E., Szabo, P., Dvořák, P., Stork, J., Krajsová, I., Dundr, P., Smetana, K., Jr and Lacina, L. (2013) Cultivation-dependent plasticity of melanoma phenotype. Tumour Biol. **34**, 3345–3355

Kolar, M., Szabo, P., Dvorankova, B., Lacina, L., Gabius, H.-J., Strnad, H., Sachova, J., Vlcek, C., Plzak, J., Chovanec, M., Cada, Z., Betka, J., Fík, Z., Pačes, J., Kovarova, H., Motlík, J., Jarkovská, K. and Smetana, K., Jr. (2012) Upregulation of IL-6, IL-8 and CXCL-1 production in dermal fibroblasts by normal/malignant epithelial cells in vitro: Immunohistochemical and transcriptomic analyses. Biol. Cell **104**, 738–751

Kowal-Vern, A. and Criswell, B.K. (2005) Burn scar neoplasms: a literature review and statistical analysis. Burns **31**, 403–413

Lazard, D., Sastre, X., Frid, M.G., Glukhova, M.A., Thiery, J.P. and Koteliansky, V.E. (1993) Expression of smooth muscle-specific proteins in myoepithelium and stromal myofibroblasts of normal and malignant human breast tissue. Proc. Natl. Acad. Sci. U.S.A. **90**, 999–1003

Leung, W.K.C., Ching, A.K.K. and Wong, N. (2011) Phosphorylation of Caldesmon by PFTAIRE1 kinase promotes actin binding and formation of stress fibers. Mol. Cell. Biochem. **350**, 201–206

Malmström, J., Lindberg, H., Lindberg, C., Bratt, C., Wieslander, E., Delander, E.-L., Särnstrand, B., Burns, J.S., Mose-Larsen, P., Fey, S. and Marko-Varga, G. (2004) Transforming growth factor-beta 1 specifically induce proteins involved in the myofibroblast contractile apparatus. Mol. Cell. Proteomics **3**, 466–477

McCormack, E.A., Altschuler, G.M., Dekker, C., Filmore, H. and Willison, K.R. (2009) Yeast phosducin-like protein 2 acts as a stimulatory co-factor for the folding of actin by the chaperonin CCT via a ternary complex. J. Mol. Biol. **391**, 192–206

Méndez, E., Cheng, C., Farwell, D.G., Ricks, S., Agoff, S.N., Futran, N.D., Weymuller, E.A., Jr, Maronian, N.C., Zhao, L.P. and Chen, C. (2002) Transcriptional expression profiles of oral squamous cell carcinomas. Cancer **95**, 1482–1494

Otranto, M., Sarrazy, V., Bonté, F., Hinz, B., Gabbiani, G. and Desmoulière, A. (2012) The role of the myofibroblast in tumor stroma remodeling. Cell Adhes. Migr. **6**, 203–219

Pho, M., Lee, W., Watt, D.R., Laschinger, C., Simmons, C.A. and McCulloch, C.A. (2008) Cofilin is a marker of myofibroblast differentiation in cells from porcine aortic cardiac valves. Am. J. Physiol. Heart Circ. Physiol. **294**, H1767–1778

Plzak, J., Lacina, L., Chovanec, M., Dvorankova, B., Szabo, P., Cada, Z. and Smetana, K., Jr. (2010) Epithelial–stromal interaction in squamous cell epithelium-derived tumors: an important new player in the control of tumor biological properties. Anticancer Res. **30**, 455–462

Polyak, K., Haviv, I. and Campbell, I.G. (2009) Co-evolution of tumor cells and their microenvironment. Trends Genet. **25**, 30–38

Radisky, D.C., Kenny, P.A. and Bissell, M.J. (2007) Fibrosis and cancer: do myofibroblasts come also from epithelial cells via EMT? J. Cell. Biochem. **101**, 830–839

Salgueiredo-Giudice, F., Fornias-Sperandio, F., Martins-Pereira, E., da Costa dal Vechio, A.M., de Sousa, S.C.O.M., and dos Santos-Pinto-Junior, D. (2011) The immunohistochemical profile of oral inflammatory myofibroblastic tumors. Oral Surg. Oral Med. Oral Pathol. Oral Radiol. Endod. **111**, 749–756

Satish, L., Johnson, S., Abdulally, A., Post, J.C., Ehrlich, G.D. and Kathju, S. (2010) Cloning and expression of rabbit CCT subunits eta and beta in healing cutaneous wounds. Cell Stress Chaperones **15**, 819–826

Schwappacher, R., Rangaswami, H., Su-Yuo, J., Hassad, A., Spitler, R. and Casteel, D.E. (2013) cGMP-dependent protein kinase I regulates breast cancer cell migration and invasion via interaction with the actin/myosin-associated protein caldesmon. J. Cell Sci. **126**, 1626–1636

Smetana, K., Jr, Dvorankova, B., Szabo, P., Strnad, H. and Kolar, M. (2013) Role of stromal fibroblasts in cancer originated from squamous epithelia. In *Dermal fibroblasts: Histological perspectives, characterization and role in disease*; Bai X, Ed. pp. 83–94

Strnad, H., Lacina, L., Kolář, M., Čada, Z., Vlček, Č., Dvořánková, B., Betka, J., Plzák, J., Chovanec, M., Šáchová, J., Urbanová, M. and Smetana, K., Jr. (2010) Head and neck squamous cancer stromal fibroblasts produce growth factors influencing phenotype of normal human keratinocytes. Histochem. Cell Biol. **133**, 201–211

Szabo, P., Valach, J., Smetana, K., Jr and Dvořánková, B. (2013) Comparative analysis of IL-8 and CXCL-1 production by normal and cancer stromal fibroblasts. Folia Biol. (Praha) **59**, 134–137

Valach, J., Fík, Z., Strnad, H., Chovanec, M., Plzák, J., Cada, Z., Szabo, P., Sáchová, J., Hroudová, M., Urbanová, M., Steffl, M., Pačes, J., Mazánek, J., Vlček, C., Betka, J., Kaltner, H., André, S., Gabius, H.J., Kodet, R., Smetana, K. Jr., Gál, P. and Kolář, M. (2012) Smooth muscle actin-expressing stromal fibroblasts in head and neck squamous cell carcinoma: increased expression of galectin-1 and induction of poor prognosis factors. Int. J. Cancer **131**, 2499–2508

De Wever, O., Demetter, P., Mareel, M. and Bracke, M. (2008) Stromal myofibroblasts are drivers of invasive cancer growth. Int. J. Cancer **123**, 2229–2238

Zhao, X.-H., Laschinger, C., Arora, P., Szászi, K., Kapus, A. and McCulloch, C.A. (2007) Force activates smooth muscle alpha-actin promoter activity through the Rho signaling pathway. J. Cell Sci. **120**, 1801–1809

Received: 12 February 2014; Accepted: 27 March 2014; Accepted article online: 2 April 2014